Available online at www.sciencedirect.com
SCIENCE DIRECT
Journal of Power Sources 147 (2005) 58–71
JOURNAL OF POWER SOURCES
www.elsevier.com/locate/jpowsour

Model for the contamination of fuel cell anode catalyst in the presence of fuel stream impurities

Jiujun Zhang [a,*], Haijiang Wang [a], David P. Wilkinson [a,b], Datong Song [a], Jun Shen [a], Zhong-Sheng Liu [a]

[a] *Institute for Fuel Cell Innovation, National Research Council Canada, Vancouver, BC, Canada V6T 1W5*
[b] *Department of Chemical and Biological Engineering, University of British Columbia, Vancouver, BC, Canada V6T 1Z4*

Received 7 December 2004; accepted 1 January 2005
Available online 18 March 2005

Abstract

A model dealing with the anode catalyst contamination induced by fuel impurities has been developed. This model can be used to describe the transient and steady-state performance losses. Several characteristics such as performance loss, contamination transient time constant and recovery process have also been introduced into the model. The obtained equations can be used to simulate and estimate the chemical and electrochemical reaction rate constants, and make some prediction about the severity of the contamination and the performance recoverability.

Keywords: Fuel cell; Anode catalyst; Contamination; Modeling

1. Introduction

Fuel cell contamination caused by the impurities in the feed stream is one of the important issues in fuel cell development and operation [1–24]. The major impurities in the hydrogen stream are CO, H_2S, NH_3, organic sulfur–carbon and carbon–hydrogen compounds, etc., produced in the hydrogen production process (for example, natural gas reforming). These impurities (or contaminants) degrade the cell performance and sometimes cause permanent membrane electrode assembly (MEA) damage. The two effects can be used to describe the contamination process: (1) kinetic effect (poisoning of the electrode catalyst) and (2) conductivity effect (increase in the solid electrolyte resistance including those of membrane and catalyst layer ionomer). It is well known and widely documented that the major impact of CO contaminant on the MEA performance is the kinetic effect that is the poisoning of the anode catalyst [1,25–27]. For H_2S contamination, the impact is also kinetic related and has also been recognized as a severe depression in the fuel cell performance for many years [1,3,12,14,18–24]. NH_3, as one of the fuel impurities, has also been investigated in fuel cell operation [2,3] and the conductivity effect has been found to be the major cause for the fuel cell degradation.

It has been found that the performance loss is related to the contaminant concentration in the feed stream [2,3], and the fuel cell operating current density (or cell voltage). In general, the higher the contaminant level or current density, the faster and deeper the depression is. For the purpose of fundamental understanding and application development, a model is necessary to describe theoretically the contamination process. For the CO poisoning process, several model papers have been published, which mainly focused on the steady-state poisoning effect [26,28–30]. For a transient process, Bhatia and Wang has reported a model and validated it by experimental results [30]. A general and complete model for the contamination process as a function of contaminant level and current density, including transient, steady-state and recovery processes, is expected to be very useful in fuel cell research and development.

* Corresponding author. Tel.: +1 604 221 3087; fax: +1 604 221 3001.
E-mail address: jiujun.zhang@nrc.gc.ca (J. Zhang).

0378-7753/$ – see front matter.
doi:10.1016/j.jpowsour.2005.01.013

Nomenclature

a	as defined in the text for the recovery process ($mol^3\ cm^{-6}\ h^{-3}$)
b	as defined in the text for the recovery process ($mol^3\ cm^{-6}\ h^{-3}$)
A	as defined in the text
A_0	as defined in the text
B	as defined in the text
B_1	sum of the rate constants ($mol\ cm^{-2}\ h^{-1}$)
B_2	backward rate for reaction (7) ($mol\ cm^{-2}\ h^{-1}$)
B_1^S	sum of the rate constants at steady-state anode overpotential ($mol\ cm^{-2}\ h^{-1}$)
B_2^S	backward rate for reaction (7) at steady-state anode overpotential ($mol\ cm^{-2}\ h^{-1}$)
C	as defined in the text
C_{H_2}	concentration of hydrogen in the electrolyte (Nafion ionomer catalyst layer) ($mol\ cm^{-3}$)
C_O	concentration of air oxygen in the electrolyte (Nafion ionomer catalyst layer) ($mol\ cm^{-3}$)
C_{H^+}	proton concentration in the catalyst layer ($mol\ cm^{-3}$)
C_P	contaminant concentration (ppm)
$C_{P'}$	contaminant reaction product concentration (ppm)
E_a	anode potential at $I_a \neq 0$ and $C_P \neq 0$ (V)
E_a^0	anode potential at $I_a = 0$ and $C_P = 0$ (V)
E^{0a}	standard anode potential (V)
E_c	cathode potential at $I_a \neq 0$ and $C_P \neq 0$ (V)
E_c^0	cathode potential at $I_a = 0$ and $C_P = 0$ (V)
F	Faraday's constant (96,487 A s mol^{-1})
F_1	sum of the forward rate constants ($mol\ cm^{-2}\ h^{-1}$)
F_2	forward rate for reaction (7) ($mol\ cm^{-2}\ h^{-1}$)
F_1^S	sum of the forward rate constants at steady-state anode overpotential ($mol\ cm^{-2}\ h^{-1}$)
F_2^S	forward rate for reaction (7) at steady-state anode overpotential ($mol\ cm^{-2}\ h^{-1}$)
$F_1^{t \geq t_0}$	sum of the forward rate constants after the contaminant is cut-off ($mol\ cm^{-2}\ h^{-1}$)
i_H^0	exchange current density for hydrogen oxidation on the platinum surface in the absence of contaminant ($A\ cm^{-2}$)
i_O^0	exchange current density for oxygen reduction on the platinum surface in the absence of contaminant ($A\ cm^{-2}$)
I_a	fuel cell anode current density ($A\ cm^{-2}$)
I_c	fuel cell cathode current density ($A\ cm^{-2}$)
I_{cell}	fuel cell operating current density ($A\ cm^{-2}$)
k_{1f}	reaction (1) forward reaction rate constant ($cm\ h^{-1}$)
k_{1b}	reaction (1) backward reaction rate constant ($mol\ cm^{-2}\ h^{-1}$)
k_{2f}	reaction (2) forward reaction rate constant ($mol\ cm^{-2}\ h^{-1}$)
k_{2b}	reaction (2) backward reaction rate constant ($mol\ cm^{-2}\ h^{-1}$)
k_{3f}	reaction (3) forward reaction rate constant ($mol\ cm^{-2}\ h^{-1}$)
k_{3b}	reaction (3) backward reaction rate constant ($cm\ h^{-1}$)
k_{4f}	reaction (4) forward reaction rate constant ($mol\ cm^{-2}\ ppm^{-1}\ h^{-1}$)
k_{4b}	reaction (4) backward reaction rate constant ($mol\ cm^{-2}\ h^{-1}$)
k_{5f}	reaction (5) forward reaction rate constant ($mol\ cm^{-2}\ ppm^{-1}\ h^{-1}$)
k_{5b}	reaction (5) backward reaction rate constant ($cm\ h^{-1}$)
k_{6f}	reaction (6) forward reaction rate constant ($mol\ cm^{-2}\ ppm^{-1}\ h^{-1}$)
k_{6b}	reaction (6) backward reaction rate constant ($cm\ h^{-1}$)
k_{7f}	reaction (7) forward reaction rate constant ($mol\ cm^{-2}\ h^{-1}$)
k_{7b}	reaction (7) backward reaction rate constant ($mol^{1-q}\ cm^{3q-2}\ h^{-1}$)
k_{8f}	reaction (8) forward reaction rate constant ($mol\ cm^{-2}\ h^{-1}$)
k_{8b}	reaction (8) backward reaction rate constant ($mol^{-q}\ cm^{3q+1}\ h^{-1}$)
m	water stoichiometry in reactions (7) and (8)
n_{α_O}	electron transfer coefficient for overall cathode oxygen reduction
n_H	electron transfer number for overall hydrogen oxidation
n_O	electron transfer number for overall cathode oxygen reduction
$n_{3,5,7-8}$	electron transfer number for individual electrochemical half-reaction
P	symbol for contaminant
P′	symbol for the product of P electrochemical oxidation
PL%	fuel cell performance loss in the presence of contaminant
R	Gas constant ($8.314\ J\ K^{-1}\ mole^{-1}$)
q	proton and electron numbers in reactions (7) and (8)
R_0	fuel cell internal resistance (electrolyte (membrane) resistance) ($\Omega\ cm^2$)
t_0	lifetime moment at which the contaminant source is cut-off (h)
T	temperature (K)
V_{cell}	fuel cell voltage (V)

$V_{\text{cell}}^{C_p=0}$ steady fuel cell voltage in the absence of contaminant (V)
V_{cell}^{S} fuel cell steady-state cell voltage in the presence of contaminant (V)
V^{o} fuel cell open circuit voltage (V)
Z as defined in the text (mol cm^{-2} h^{-1})
$Z^{t\geq t_0}$ as defined in the text (mol cm^{-2} h^{-1})

Greek symbols
$\alpha_{3,5,7-8}$ electron transfer coefficient for individual electrochemical half-reaction
α_{O} electron transfer coefficient for fuel cell cathode oxygen reduction
γ_a real active surface-to-electrode geometric surface ratio of the anode catalyst layer (cm^2 cm^{-2})
γ_c real active surface-to-electrode geometric surface ratio of the cathode catalyst layer (cm^2 cm^{-2})
Γ_{Pt} Pt surface site concentration (mol cm^{-2})
Γ_{Pt-H} Pt surface site concentration (mol cm^{-2})
Γ_{Pt-H_2} Pt surface site concentration (mol cm^{-2})
Γ_{Pt-P} Pt surface site concentration (mol cm^{-2})
$\Gamma_{Pt-P'}$ Pt surface site concentration (mol cm^{-2})
Γ_{Pt}^{T} total surface site concentration (mol cm^{-2})
η_a anode overpotential (V)
η_c cathode overpotential (V)
θ_{Pt} surface coverage of platinum unoccupied site
θ_{Pt}^{0} surface coverage of platinum unoccupied site at equilibrium anode potential
θ_{Pt-H} surface coverage of hydrogen atom on the platinum
θ_{Pt-H}^{0} hydrogen atom surface coverage on platinum at equilibrium anode potential
θ_{Pt-H_2} hydrogen molecule surface coverage on the platinum
θ_{Pt-P} contaminant surface coverage on the platinum
$\theta_{Pt-P'}$ contaminant reaction product surface coverage on the platinum
$\theta_{Pt-P}^{t\geq t_0}$ contaminant surface coverage on the platinum after the contaminant source is cut-off
$\theta_{Pt-P'}^{t\geq t_0}$ contaminant reaction product surface coverage on the platinum after the contaminant source is cut-off
$\theta_{Pt-P}^{t=t_0}$ contaminant surface coverage on the platinum at the moment of $t = t_0$
$\theta_{Pt-P'}^{t=t_0}$ contaminant reaction product surface coverage on the platinum at the moment of $t = t_0$
τ contamination transient time constant (h)

In this paper, only the kinetic effects will be considered in the modeling process. Thus, a model dealing with the general case of anode catalyst contamination by fuel impurities has been developed. This model can be used to describe the transient and steady-state performance loss processes. Several characteristic parameters such as performance loss, contamination transient time constant, and recovery period have also been introduced to describe the contamination/recovery processes.

2. Model description

2.1. Proposed anode chemical reactions in the presence of contaminant P

In order to simulate the degradation behavior of the cell performance in the presence of a stream contaminant, and determine quantitatively the relationship of contamination surface coverage as a function of the contaminant concentration, cell current density and lifetime, several possible chemical and electrochemical reactions with their corresponding reaction constants have been assumed, as in reactions (I)–(VIII):

$$\text{Pt} + \text{H}_2 \underset{k_{1b}}{\overset{k_{1f}}{\rightleftarrows}} \text{Pt–H}_2 \quad \text{(I)}$$

$$\text{Pt–H}_2 + \text{Pt} \underset{k_{2b}}{\overset{k_{2f}}{\rightleftarrows}} 2\text{Pt–H} \quad \text{(II)}$$

$$\text{Pt–H} \underset{k_{3b}\ \exp(-(1-\alpha_3)n_3F\eta_a/RT)}{\overset{k_{3f}\ \exp(\alpha_3 n_3 F\eta_a/RT)}{\rightleftarrows}} \text{Pt} + \text{H}^+ + \text{e}^- \quad \text{(III)}$$

$$\text{P} + \text{Pt} \underset{k_{4b}}{\overset{k_{4f}}{\rightleftarrows}} \text{Pt–P} \quad \text{(IV)}$$

$$\text{P} + \text{Pt–H} \underset{k_{5b}\ \exp(-(1-\alpha_5)n_5F\eta_a/RT)}{\overset{k_{5f}\ \exp(\alpha_5 n_5 F\eta_a/RT)}{\rightleftarrows}} \text{Pt–P} + \text{H}^+ + \text{e}^- \quad \text{(V)}$$

$$\text{P} + \text{Pt–H}_2 \underset{k_{6b}}{\overset{k_{6f}}{\rightleftarrows}} \text{Pt–P} + \text{H}_2 \quad \text{(VI)}$$

$$\text{Pt–P} + m\text{H}_2\text{O} \underset{k_{7b}\ \exp(-(1-\alpha_7)qF\eta_a/RT)}{\overset{k_{7f}\ \exp(\alpha_7 qF\eta_a/RT)}{\rightleftarrows}} \text{Pt–P}' + q\text{H}^+ + q\text{e}^- \quad \text{(VII)}$$

$$\text{Pt–P} + m\text{H}_2\text{O} \underset{k_{8b}\ \exp(-(1-\alpha_8)qF\eta_a/RT)}{\overset{k_{8f}\ \exp(\alpha_8 qF\eta_H/RT)}{\rightleftarrows}} \text{Pt} + \text{P}' + q\text{H}^+ + q\text{e}^- \quad \text{(VIII)}$$

Reactions (I)–(III) are the mechanism for hydrogen oxidation, which has been investigated and reported for many years [25,26,31–44]. Reaction (I) is the adsorption of H_2 on the platinum surface, which is a fast reaction. Reaction (II) is the slow dissociative chemical adsorption of adsorbed H_2,

which has been considered as the rate-determining step for H_2 oxidation [25,26] and reaction (III) is the fast electrochemical oxidation of the dissociated hydrogen atom. Reactions (IV)–(VI) are those surface adsorption and surface electrochemical reaction of the poisoning species (marked as P). Note that reactions (V) and (VI) proposed here are used to describe the interaction between the contaminant species P and the atomic and molecular hydrogen occupied Pt surface. It is worthwhile to point out that in some situations, one contaminant P molecule could react with several surface Pt atoms to form surface species such as Pt_n–P (i.e., $n \geq 1$). However, in order to make the modeling process simpler, only Pt–P is considered as the surface poisoning species in this paper. Reaction (VII) or (VIII) is the oxidation of adsorbed contaminant on the Pt surface, resulting in a product that could be either a surface adsorbed species (Pt–P′) or a soluble species (P′). In the case that P is not electrochemically reactive, the corresponding reactions (VII) and (VIII) would be removed from the proposed mechanism. Each reaction has its own rate constants (k_{if} for forward and k_{ib} for backward). For those electrochemical reactions (reactions (III), (V), (VII) and (VIII)), the rate constants are electrode overpotential dependent, and written according to the Butler–Volmer equation. Where α_i, n_i and q are electron transfer coefficient, electron transfer number and the proton/electron numbers for the corresponding electrochemical reaction.

2.2. Surface coverage and their expressions as a function of anode overpotential

The anode overpotential is the difference between two stages of anode potential, i.e., the anode equilibrium state potential (E_a^0) at which the anode net current density (I_a) and the contaminant concentration (C_P) are both equal to zero, and the anode potential (E_a) at which both I_a and C_P are not equal to zero, that is, $\eta_a = E_a - E_a^0$. In order to obtain the time dependence of contaminant surface coverage, the interrelationship among various kinds of surface coverage and the anode overpotential have to be obtained. As in the reaction mechanism proposed above, there are five kinds of surface sites, which are Pt, Pt–H_2, Pt–H, Pt–P and Pt–P′. Their corresponding surface concentration can be expressed as Γ_{Pt}, Γ_{Pt-H}, Γ_{Pt-H_2}, Γ_{Pt-P}, and $\Gamma_{Pt-P'}$ with a unit of mol cm^{-2}. The sum of these surface concentrations can be defined as the total available Pt surface concentration, Γ_{Pt}^T with a unit of mol cm^{-2}. The surface coverage for each surface site can be expressed as θ_{Pt} ($=\Gamma_{Pt}/\Gamma_{Pt}^T$), θ_{Pt-H}($=\Gamma_{Pt-H}/\Gamma_{Pt}^T$), θ_{Pt-H_2}($=\Gamma_{Pt-H_2}/\Gamma_{Pt}^T$), θ_{Pt-P}($=\Gamma_{Pt-P}/\Gamma_{Pt}^T$) and $\theta_{Pt-P'}$($=\Gamma_{Pt-P'}/\Gamma_{Pt}^T$), respectively. Fig. 1 shows the schematic expression of a platinum surface with different surface sites.

The equation (1) can be used to describe the interrelationship among the surface coverage terms:

$$\theta_{Pt} + \theta_{Pt-H} + \theta_{Pt-H_2} + \theta_{Pt-P} + \theta_{Pt-P'} = 1 \quad (1)$$

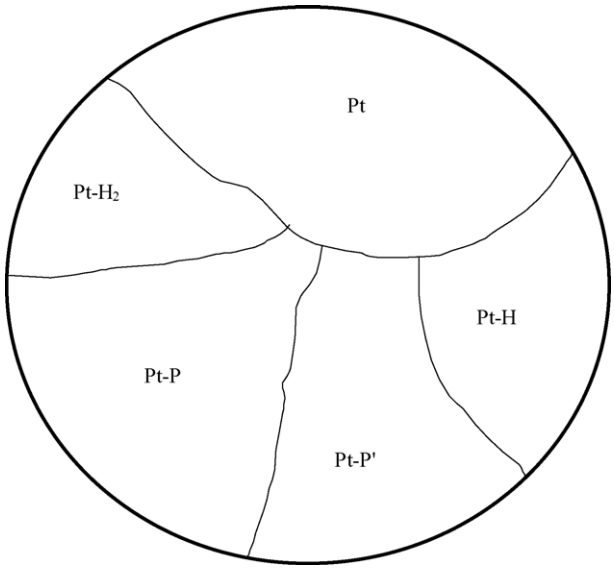

Fig. 1. Schematic diagram of a platinum surface with adsorption of molecular hydrogen, atomic hydrogen, contaminant and contaminant reaction product.

At anode equilibrium potential in the absence of contaminant, equation (2) can be used to describe the surface coverage:

$$\theta_{Pt}^0 + \theta_{Pt-H}^0 + \theta_{Pt-H_2}^0 = 1 \quad (2)$$

Since reaction (II) is the rate-determining step, it can be assumed that reaction (I) is always at its equilibrium state whether there is a contaminant present or not. From reaction (I), the relationship between θ_{Pt} and θ_{Pt-H_2} can be established:

$$\theta_{Pt-H_2} = \frac{k_{1f}}{k_{1b}} C_{H_2} \theta_{Pt} \quad (3)$$

where C_{H_2} is the average concentration of hydrogen in the vicinity of the catalyst layer, expressed either by gas concentration or the wet concentration in the electrolyte (ionomer matrix layer in the catalyst layer, mol cm^{-3}).

If reaction (III) is very fast, the anode potential would follow the Nernst behavior even in the presence of poisoning species [25,26]:

$$E_a = E^{0a} + \frac{RT}{F} \ln\left(\frac{k_{3b}}{k_{3f}}\right) + \frac{RT}{F} \ln\left(\frac{\theta_{Pt} C_{H^+}}{\theta_{Pt-H}}\right) \quad (4)$$

where E^{0a} is the standard anode potential of the hydrogen redox reaction and C_{H^+} is the concentration of proton. At zero current density (reaction (III) at its equilibrium state), and if the contaminant species P is absent, the equilibrium electrode potential would be:

$$E_a^0 = E^{0a} + \frac{RT}{F} \ln\left(\frac{k_{3b}}{k_{3f}}\right) + \frac{RT}{F} \ln\left(\frac{\theta_{Pt}^0 C_{H^+}}{\theta_{Pt-H}^0}\right) \quad (5)$$

where θ^0_{Pt} and θ^0_{Pt-H} are the surface coverage at equilibrium anode potential in the absence of the contaminant. Combining equations (1)–(5), the surface coverage of hydrogen molecules, hydrogen atoms and unoccupied Pt sites can be expressed as a function of anode overpotential η_a and contaminant coverage θ_{Pt-P} and $\theta_{Pt-P'}$:

$$\theta_{Pt} = A(1 - \theta_{Pt-P} - \theta_{Pt-P'}) \tag{6}$$

where

$$A = \frac{\frac{\theta^0_{Pt}}{\theta^0_{Pt-H}} \exp\left(\frac{F\eta_a}{RT}\right)}{1 + \frac{\theta^0_{Pt}}{\theta^0_{Pt-H}}\left(1 + \frac{k_{1f}}{k_{1b}}C_{H_2}\right)\exp\left(\frac{F\eta_a}{RT}\right)},$$

$$\theta_{Pt-H_2} = B(1 - \theta_{Pt-P} - \theta_{Pt-P'}) \tag{7}$$

where $B = \frac{k_{1f}}{k_{1b}}C_{H_2}A$, and

$$\theta_{Pt-H} = C(1 - \theta_{Pt-P} - \theta_{Pt-P'}) \tag{8}$$

where $C = 1 - \left(1 + \frac{k_{1f}}{k_{1b}}C_{H_2}\right)A$.

The surface coverage ratio in equation (6), $\theta^0_{Pt}/\theta^0_{Pt-H}$, is determined by the equilibrium anode potential and proton concentration as shown in equation (5).

2.3. Contaminant surface coverage as a function of η_a and lifetime (t)

From reaction (IV) to (VII), the increase in contaminant surface coverage with time can be written as equations (9) and (9′) according to the chemical reaction rate laws:

$$\begin{aligned}
&\Gamma^T_{Pt}\frac{d(\theta_{Pt-P})}{dt} \\
&= k_{4f}C_P\theta_{Pt} - k_{4b}\theta_{Pt-P} + k_{5f}C_P\theta_{Pt-H}\exp\left(\frac{\alpha_5 n_5 F\eta_a}{RT}\right) \\
&\quad - k_{5b}C_{H^+}\theta_{Pt-P}\exp\left(-\frac{(1-\alpha_5)n_5F\eta_a}{RT}\right) \\
&\quad + k_{6f}C_P\theta_{Pt-H_2} - k_{6b}\theta_{Pt-P}C_{H_2} - k_{7f}\theta_{Pt-P} \\
&\quad \times \exp\left(\frac{\alpha_7 qF\eta_a}{RT}\right) + k_{7b}C^q_{H+}\theta_{Pt-P'} \\
&\quad \times \exp\left(-\frac{(1-\alpha_7)qF\eta_a}{RT}\right) - k_{8f}\theta_{Pt-P}\exp\left(\frac{\alpha_8 qF\eta_a}{RT}\right) \\
&\quad + k_{8b}C_{P'}C^q_{H^+}\theta_{Pt}\exp\left(-\frac{(1-\alpha_8)qF\eta_a}{RT}\right)
\end{aligned} \tag{9}$$

$$\Gamma^T_{Pt}\frac{d(\theta_{Pt-P'})}{dt} = k_{7f}\theta_{Pt-P}\exp\left(\frac{\alpha_7 qF\eta_a}{RT}\right) - k_{7b}C^q_{H^+}\theta_{Pt-P'} \times \exp\left(-\frac{(1-\alpha_7)qF\eta_a}{RT}\right) \tag{9'}$$

Substituting equations (6)–(8) into equation (9) for θ_{Pt}, θ_{Pt-H} and θ_{Pt-H_2} will result in an equation (10) which only contains θ_{Pt-P} and $\theta_{Pt-P'}$ as the surface coverage:

$$\begin{aligned}
&\Gamma^T_{Pt}\frac{d(\theta_{Pt-P})}{dt} \\
&= A\left[k_{4f}C_P + k_{8b}C_{P'}C^q_{H^+}\exp\left(-\frac{(1-\alpha_8)qF\eta_a}{RT}\right)\right] \\
&\quad + Bk_{6f}C_P + Ck_{5f}C_P\exp\left(\frac{\alpha_5 n_5 F\eta_a}{RT}\right) \\
&\quad - \left\{A\left[k_{4f}C_P + k_{8b}C_{P'}C^q_{H^+}\exp\left(\frac{-(1-\alpha_8)qF\eta_a}{RT}\right)\right]\right. \\
&\quad + Bk_{6f}C_P + Ck_{5f}C_P\exp\left(\frac{\alpha_5 n_5 F\eta_a}{RT}\right) + k_{4b} \\
&\quad + K_{5b}C_{H^+}\exp\left(\frac{-(1-\alpha_5)n_5F\eta_a}{RT}\right) + k_{6b}C_{H_2} + k_{8f}\exp \\
&\quad \left.\times\left(\frac{\alpha_8 qF\eta_a}{RT}\right) + k_{7f}\exp\left(\frac{\alpha_7 qF\eta_a}{RT}\right)\right\}\theta_{Pt-P} \\
&\quad - \left\{A\left[k_{4f}C_P + k_{8b}C_{P'}C^q_{H^+}\exp\left(\frac{-(1-\alpha_8)qF\eta_a}{RT}\right)\right]\right. \\
&\quad + Bk_{6f}C_P + Ck_{5f}C_P\exp\left(\frac{\alpha_5 n_5 F\eta_a}{RT}\right) - k_{7b}C^q_{H^+}\exp \\
&\quad \left.\times\left(\frac{-(1-\alpha_7)qF\eta_a}{RT}\right)\right\}\theta_{Pt-P'}
\end{aligned} \tag{10}$$

The differential equations (10) and (9′) can be solved with the boundary conditions of that at $t = 0$, θ_{Pt-P} and $\theta_{Pt-P'} = 0$, and C_P and $C_{P'} = 0$. The contaminant surface coverage can be obtained as a function of contaminant concentration, anode overpotential and the lifetime, as expressed by equations (11) and (11′):

$$\begin{aligned}
&\theta_{Pt-P} \\
&= \frac{F_1}{F_1F_2 + F_1B_2 + B_1B_2} \\
&\quad \times\left[B_2 - \frac{1}{2}\left(B_2 - \frac{F_1B_2 + B_1B_2 - B_2B_2 + 2F_1F_2 - F_2B_2}{Z}\right)\right. \\
&\quad \times\exp\left(-\frac{F_1 + B_1 + F_2 + B_2 - Z}{2}t\right) \\
&\quad -\frac{1}{2}\left(B_2 + \frac{F_1B_2 + B_1B_2 - B_2B_2 + 2F_1F_2 - F_2B_2}{Z}\right) \\
&\quad \left.\times\exp\left(-\frac{F_1 + B_1 + F_2 + B_2 + Z}{2}t\right)\right]
\end{aligned} \tag{11}$$

$$\begin{aligned}
&\theta_{Pt-P'} \\
&= \frac{F_1}{F_1F_2 + F_1B_2 + B_1B_2} \\
&\quad \times\left[F_2 + \frac{1}{2}\left(B_2 - \frac{F_1B_2 + B_1B_2 - B_2B_2 + 2F_1F_2 - F_2B_2}{Z}\right)\right.
\end{aligned}$$

$$\times \left(\frac{F_1+B_1+F_2-B_2+Z}{2(F_1-B_2)}\right)$$
$$\times \exp\left(-\frac{F_1+B_1+F_2+B_2-Z}{2}t\right)$$
$$+\frac{1}{2}\left(B_2+\frac{F_1B_2+B_1B_2-B_2B_2+2F_1F_2-F_2B_2}{Z}\right)$$
$$\times \left(\frac{F_1+B_1+F_2-B_2-Z}{2(F_1-B_2)}\right)$$
$$\times \exp\left(-\frac{F_1+B_1+F_2+B_2+Z}{2}t\right)\Bigg] \quad (11')$$

where

$$F_1 = A\left[k_{4f}C_P + k_{8b}C_{P'}C_{H^+}^2 \exp\left(\frac{-(1-\alpha_7)qF\eta_a}{RT}\right)\right] + Bk_{6f}C_P$$
$$B_1 = k_{4b} + k_{5b}C_{H^+} \exp\left(\frac{-(1-\alpha_5)n_5F\eta_a}{RT}\right) + k_{6b}C_{H_2} + k_{7f}\exp\left(\frac{\alpha_7qF\eta_a}{RT}\right) + k_{8f}\exp\left(\frac{\alpha_8qF\eta_a}{RT}\right)$$
$$F_2 = k_{7f}\exp\left(\frac{\alpha_7qF\eta_a}{RT}\right)$$
$$B_2 = k_{7b}C_{H^+}^q \exp\left(\frac{-(1-\alpha_7)qF\eta_a}{RT}\right)$$
$$Z = \sqrt{(F_1+F_2+B_1-B_2)^2 - 4F_2(F_1-B_2)} \quad (11'')$$

In equation (11″), F_1 represents the sum of the rate constants of the forward direction for the reactions (IV)–(VI). These forward direction reactions are mainly responsible for the production of Pt–P. B_1 represents the sum of the reaction constants whose corresponding reactions ((IV)–(VI) and (VIII)) will result in the decrease in the surface coverage of Pt–P. F_2 is the forward rate constant of the reaction (VII) which is responsible for the increase in the surface coverage of species Pt–P′ and partially for the decrease in the surface coverage of species Pt–P. B_2 is the backward rate constant of the reaction (VII) which is the only contributor to the decrease in the surface coverage of species Pt–P′. Z in (11) and (11′) is a special parameter for solving the differential equations. It can be proven mathematically that Z's value is always larger than zero if F_1, B_1, F_2 and B_2 all have non-zero values which is the case proposed above. However, if $F_1 = B_2$ (could be a possible case for the reaction mechanism), equation (11) will become meaningless (a number divided by zero). If this case happens, another two equations (12) and (12′) rather than equations (11) and (11′) have to be used to obtain the surface coverage:

$$\theta_{Pt-P} = \frac{F_1}{F_1+B_1+F_2}[1 - F_1\exp(-(F_1+B_1+F_2)t)] \quad (12)$$

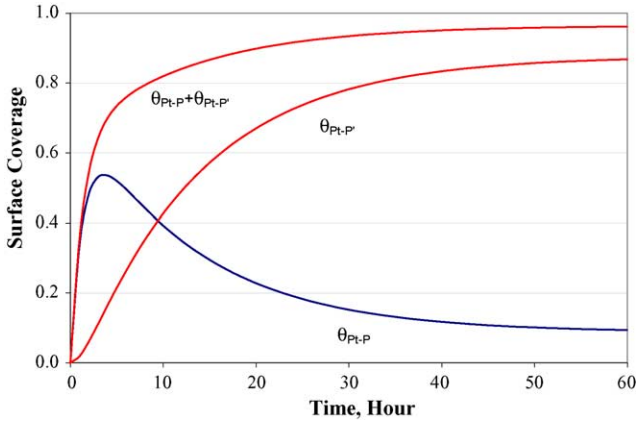

Fig. 2. Calculated surface coverage distribution of contaminant P and its oxidation product P′ on the platinum surface. The parameter values used are: $F_1 = 0.5$, $B_1 = 0.2$, $F_2 = 0.1$, and $B_2 = 0.01$ (the unit for F_1, B_1, F_2 or B_2 is mol cm^{-2} h^{-1}).

$$\theta_{Pt-P'} = \frac{F_2}{F_1+B_1+F_2} \times \left[1 + \frac{F_1}{B_1+F_2}\exp(-(F_1+B_1+F_2)t) - \frac{F_1+B_1+F_2}{B_1+F_2}\exp(-F_1t)\right] \quad (12')$$

In Appendix A, a general mathematical discussion about the conditions under which $Z = 0$ and/or $F_1 = B_2$ can be found. Although several cases are impossible from a reaction physics standpoint, the discussion is still necessary for understanding.

As an example, Fig. 2 shows the calculated distribution of the surface coverage, θ_{Pt-P}, $\theta_{Pt-P'}$ and $\theta_{Pt-P} + \theta_{Pt-P'}$ based on parameter values of $F_1 = 0.5$, $B_1 = 0.2$, $F_2 = 0.1$, and $B_2 = 0.01$ (the unit for F_1, B_1, F_2 or B_2 is mol cm^{-2} h^{-1}). It can be seen that at the early stage, both θ_{Pt-P} and $\theta_{Pt-P'}$ increases with time. After a while, θ_{Pt-P} will gradually drop and $\theta_{Pt-P'}$ will continue to increase till both reach steady-state levels. The drop of θ_{Pt-P} and the continuous rising of $\theta_{Pt-P'}$ reflect the surface electrochemical conversion from species Pt–P to Pt–P′. The magnitude of the steady-state levels is determined by the magnitude of the back reaction constant (B_1 and B_2) of the reactions. When the time is long enough, the surface will be largely covered by Pt–P and Pt–P′, that is, the sum of θ_{Pt-P} and $\theta_{Pt-P'}$ is close to 1. The remaining surface available for H_2 electrochemical oxidation would be only $1 - \theta_{Pt-P} - \theta_{Pt-P'}$, which is a very small portion of the whole anode surface. The magnitude of $1 - \theta_{Pt-P} - \theta_{Pt-P'}$ is also mainly determined by the value of the sum of $B_1 + B_2$.

In the case that P′ produced by the electrochemical oxidation of contaminant P is not adsorbed (or has very week adsorption) on the platinum surface, the surface coverage of species P′ will be equal to zero and the corresponding items related to reaction (VII) will disappear from the equation (9).

Solving the only differential equation (9) will result in a simpler expression for surface coverage θ_{Pt-P}:

$$\theta_{Pt-P} = \frac{F_1}{F_1 + B_1}[1 - \exp(-(F_1 + B_1)t)] \quad (13)$$

A typical example for this case may be the contaminant CO in the hydrogen stream where the adsorption of product CO_2 on the platinum is negligible [25–30].

For anode H_2 oxidation ($H_2 \rightarrow 2H^+ + 2e^-$), as discussed above, reaction (II) may be considered as the rate-determining step. The current density (I_a) for reaction (II) on the available catalyst Pt surface could be expressed as equation (14) [25,26]:

$$I_a = n_H F \gamma_a (k_{2f}\theta_{Pt-H_2}\theta_{Pt} - k_{2b}\theta^2_{Pt-H}) \quad (14)$$

Combining equations (6)–(8) and (14), the expression for fuel cell anode current density can be obtained:

$$I_a = n_H F \gamma_a k_{2f} \frac{k_{1f}}{k_{1b}} C_{H_2} \times \left\{ A^2 - \frac{A_0^2}{\left[1 - \left(1 + \frac{k_{1f}}{k_{1b}} C_{H_2}\right) A_0\right]^2} \times \left[1 - \left(1 + \frac{k_{1f}}{k_{1b}} C_{H_2}\right) A\right]^2 \right\} (1 - \theta_{Pt-P} - \theta_{Pt-P'})^2 \quad (14')$$

where I_a is the fuel cell anode current density and γ_a is the ratio between the real Pt surface and the geometric surface area (cm^2 Pt cm^{-2} electrode) for the fuel cell anode catalyst layer. For a fuel cell electrode reaction, the reaction zone is a three-dimensional porous catalyst layer. If we assume that the anode hydrogen oxidation is totally controlled by the kinetics (interface diffusion of reactants not considered), a simple approach is to introduce a parameter to reflect the contribution of the real catalyst reaction area to the current density. A_0 is the value of A expressed by equation (6) at the equilibrium electrode potential ($\eta_a = 0$), which could be expressed as:

$$A_0 = \frac{\frac{\theta^0_{Pt}}{\theta^0_{Pt-H}}}{1 + \frac{\theta^0_{Pt}}{\theta^0_{Pt-H}}\left(1 + \frac{k_{1f}}{k_{1b}} C_{H_2}\right)}.$$

It is worthwhile to mention here that for a fuel cell polarization, a flooded-agglomerate model has been employed to describe the relationship between the current density and the overpotential [32–34]. The detail of this model will not be pursued in this paper.

For the cathode side in the absence of the contaminant, the relationship between the current density (I_c) and the cathode potential (η_c) can be given by equation (15) for fuel cell oxygen reduction ($O_2 + 4e^- + 4H^+ \leftrightarrow 2H_2O$):

$$I_c = \gamma_c i^0_O \left[\exp\left(\frac{\alpha_O n_{\alpha_O} F \eta_c}{RT}\right) - \exp\left(\frac{-(1-\alpha_O) n_{\alpha_O} F \eta_c}{RT}\right)\right] \quad (15)$$

Table 1
Parameters and their corresponding values for fuel cell performance calculation in the absence and presence of anode stream contaminant at 80 °C and 3 atm

Parameter	Value
n_H	2.0
F	96487 C mol^{-1}
γ_a	30000 cm^2 cm^{-2}
R	8.314 J K mol^{-1}
T	353 K
n_O	4.0
$\gamma_c i^0_o$	5.1×10^{-4} A cm^{-2}
$\alpha_O n_{\alpha_O}$	0.5
V^0	1.17 V
R^0	0.1 Ω cm^2
$k_{1f}C_{H_2}/k_{1b}$	0.1
$\theta^0_{Pt}/\theta^0_{Pt-H}$	2.0
k_{2f}	4.4×10^{-9} mol cm^{-2} h^{-1}
k_{4f}	5.0×10^{-2} mol cm^{-2} ppm^{-1} h^{-1}
k_{4b}	6.4×10^{-2} mol cm^{-2} h^{-1}
k_{5f}	4.0×10^{-1} mol cm^{-2} ppm^{-1} h^{-1}
k_{5b}	1.0×10^{-2} cm h^{-1}
k_{6f}	1.0×10^{-5} mol cm^{-2} ppm^{-1} h^{-1}
$k_{6b}C_{H_2}$	1.0×10^{-5} mol cm^{-2} h^{-1}
k_{7f}	0.0 mol cm^{-2} h^{-1}*
k_{7b}	0.0 mol^{1-q} cm^{3q-2} h^{-1}*
k_{8f}	8.0×10^{-8} mol cm^{-2} h^{-1}
k_{8b}	0.0 mol^{-q} cm^{3q+1} h^{-1}*
$\alpha_{3,5,7-8}$	0.5
n_5	1.0
q	2.0

* Assuming the corresponding reaction's contribution is negligible.

Given that the overpotential for oxygen reduction is relatively large (>60 mV), a Tafel equation can be employed to describe the cathode polarization:

$$\eta_c = \frac{RT}{\alpha_O n_{\alpha_O} F}[\ln(I_c) - \ln(\gamma_c i^0_O)] \quad (16)$$

where the electron transfer coefficient α_O and the electron transfer number n_{α_O} should be those for the rate-determining step of oxygen reduction mechanism. i^0_O is the exchange current density of oxygen reduction and the γ_c is the ratio between the real Pt surface and the geometric surface area for the cathode Pt catalyst layer. The cathode overpotential, η_c, is defined as the difference between the cathode potential (E_c) at $I_c \neq 0$ and the equilibrium potential (E^0_c) at $I_c = 0$, that is, $\eta_c = E^0_c - E_c$.

The relationship between the current density and the overpotential has been calculated according to the parameter values listed in Table 1 for the case in the absence of contaminant ($\theta_{Pt-P} + \theta_{Pt-P'} = 0$). Kinetic constants were chosen which gave a reasonable fit and trend to experimental data reported in the literature. More detailed experimental results

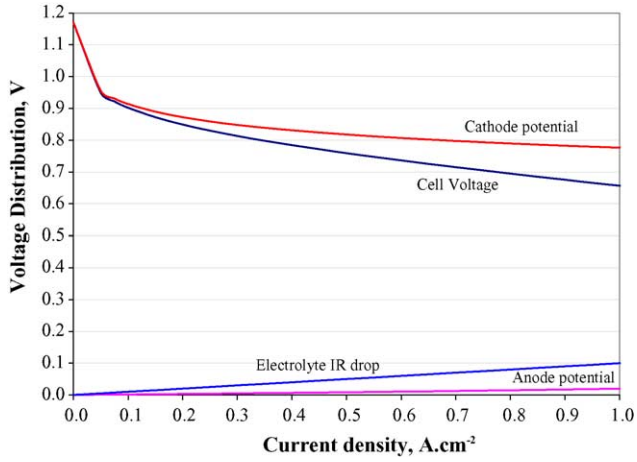

Fig. 3. Calculated fuel cell performance and corresponding voltage losses of the anode, cathode, and membrane according to the parameter values listed in Table 1 using equations (14), (16) and (17) (80 °C, 3.0 atm).

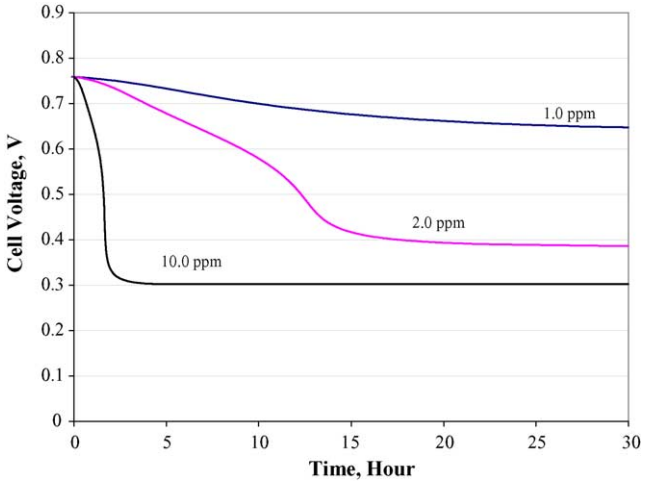

Fig. 4. Calculated fuel cell voltage degradation in the presence of various levels of the fuel stream contaminant at 80 °C, 3.0 atm and a current density of 0.5 A cm^{-2}. The reaction rate constants and other related parameters used for this calculation are those listed in Table 1.

for the contamination of the anode catalyst will be acquired in the next phase of research. In order to obtain the overall fuel cell performance, another parameter, R_0 the internal resistance of the cell is also listed in Table 1. Ignoring mass transport effects, the overall cell performance can be calculated according to equation (17):

$$V_{\text{cell}} = V^{\text{o}} - \eta_{\text{a}} - \eta_{\text{c}} - R_0 I_{\text{cell}} \quad (17)$$

where V_{cell} is the fuel cell voltage, V^{o} the open circuit voltage and I_{cell} is the current density. The calculated overall fuel cell performance is shown in Fig. 3 together with the anode, and cathode polarizations, and ohmic loss. This compares well with other performance related data in the literature [10,45].

Substituting equations (11) and (11′) into equation (14) for $\theta_{\text{Pt–P}}$ and $\theta_{\text{Pt–P}'}$, the anode overpotential as a function of time, current density, and contaminant concentration in the presence of contaminant can be obtained. If combining equations (14), (16), and (17), (11) and (11′), the transient fuel cell voltage in the presence of contaminant can be simulated by adjusting reaction constants k_{if}, k_{ib}, $\theta^0_{\text{Pt}}/\theta^0_{\text{Pt–H}}$ and probably α_i if the current density, anode overpotential and contaminant concentration are experimentally known. This simulation based on the measured cell voltage transient behavior can also provide a method to estimate the chemical and electrochemical kinetic constants.

Note that the resultant transient anode overpotential (η_{a}) and cell voltage (V_{cell}) expressions are the implicit functions of anode overpotential. It is difficult to get an analytical expression for η_{a} or V_{cell}. Therefore, some numerical calculations are necessary in order to obtain the transient behavior. As examples, for a simple case where $\theta_{\text{Pt–P}'} = 0$, Fig. 4 shows the calculated results at various stream contaminant concentrations based on equation (13) and Fig. 5 for those at various current densities. The parameters used for Figs. 4 and 5 are those listed in Table 1.

From the calculated Figs. 4 and 5, it can be seen that the cell performance will decrease in the presence of anode feed stream contaminant until a steady-state performance is reached. The greater the concentration of the fuel stream contaminant, the greater the rate of decrease, and loss in performance will be, and the sooner steady-state performance is reached. The effect of current density is similar to contaminant concentration. The fuel cell voltage degradation trends in the presence of fuel stream contaminants compare well with other reported data in the literature [27,29,30,46]. Again, more detailed experimental results for voltage degradation will be acquired in the next phase of research.

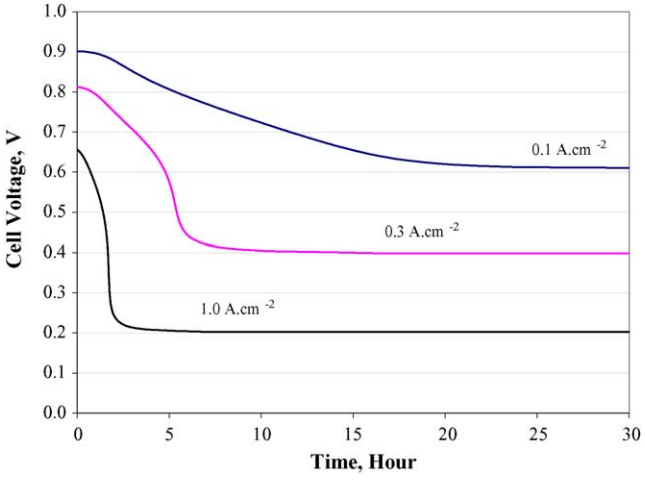

Fig. 5. Calculated fuel cell voltage degradation at various current densities in the presence of 5.0 ppm contaminant in the fuel stream at 80 °C and 3 atm. The reaction rate constants and other related parameters used for this calculation are those listed in Table 1.

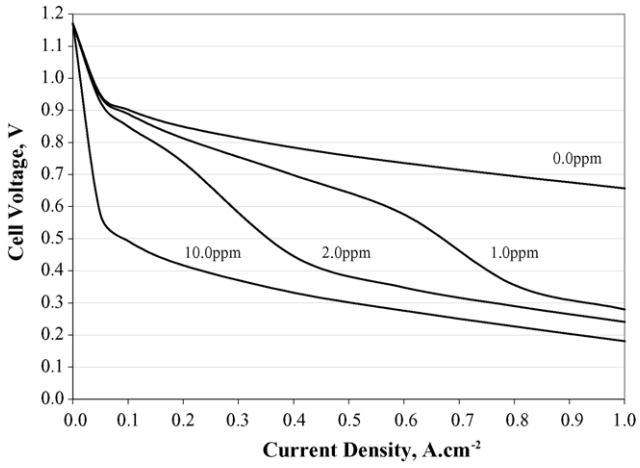

Fig. 6. Calculated fuel cell steady-state performance as a function of fuel contaminant concentration and current density at 80 °C and 3.0 atm. The parameter values used for the calculation are those listed in Table 1.

2.4. Steady-state performance in the presence of contaminant

Figs. 4 and 5 shows that there exists a steady-state performance for each contaminant concentration and current density when the lifetime goes to infinity. A steady anode overpotential and performance can be solved numerically according to the expression of steady-state surface coverage obtained through equations (11) and (11′) at $t \to \infty$:

$$(1 - \theta_{\mathrm{Pt-P}} - \theta_{\mathrm{Pt-P'}})_{t=\infty} = \frac{B_1^{\mathrm{S}} B_2^{\mathrm{S}}}{F_1^{\mathrm{S}} F_2^{\mathrm{S}} + F_1^{\mathrm{S}} B_2^{\mathrm{S}} + B_1^{\mathrm{S}} B_2^{\mathrm{S}}} \tag{18}$$

where F_1^{S}, F_2^{S}, B_1^{S} and B_2^{S} are the previous defined parameters but at steady-state under the condition of $t \to \infty$. Fig. 6 shows the calculated steady-state polarization of a fuel cell at various contaminant levels. The parameters used for Fig. 6 are those listed in Table 1. It can be observed from Fig. 6 that the steady-state performance level is a function of contaminant concentration and current density (or overpotential) as mentioned above.

Note that if the rate constant of reaction (VII) is very larger (larger F_2) or the sum of the backward rate constant is negligible ($B_1 = 0$), there will be no steady-state performance which can be observed due to the entire catalyst surface being totally occupied by P + P′ (that is, $1 - \theta_{\mathrm{Pt-P}} - \theta_{\mathrm{Pt-P'}} \approx 0$). In this case, the cell voltage and the current density will both drop to zero.

For a special case where the reaction (VII) does not exist, the equation (18) will become equation (19):

$$(1 - \theta_{\mathrm{Pt-P}} - \theta_{\mathrm{Pt-P'}})_{t=\infty} = \frac{B_1^{\mathrm{S}}}{F_1^{\mathrm{S}} + B_1^{\mathrm{S}}} \tag{19}$$

A performance loss parameter (PL%) in the presence of contaminant can be defined as equation (20):

$$\mathrm{PD\%} = 100 \left(\frac{V_{\mathrm{cell}}^{C_{\mathrm{P}}=0} - V_{\mathrm{cell}}^{\mathrm{S}}}{V_{\mathrm{cell}}^{C_{\mathrm{P}}=0}} \right) \tag{20}$$

Where $V_{\mathrm{cell}}^{\mathrm{S}}$ is the steady-state cell perfomance, and $V_{\mathrm{cell}}^{C_{\mathrm{P}}=0}$ is the steady-state cell performance in the absence of contamination.

2.5. Contamination transient time constant

A transient time constant for the contamination process can be defined as τ, which is a measure of how long it takes the performance to approximately reach its steady-state level. The expression for τ could be defined by equation (21):

$$\tau = \frac{1}{F_1 + B_1 + F_2 + B_2} \tag{21}$$

It can be observed from equations (11), (11′) that the transient time constant is a function of contaminant level and anode overpotential (or current density). In general, the higher the contaminant concentration or current density, the shorter the transient time.

2.6. Performance recovery process

It has been observed experimentally that during the contamination process, the fuel cell performance could be recovered automatically with time when the contaminant source was cut off [2,3]. One assumes that the contaminant source is switched off at a time of t_0, the boundary condition for solving equation (10) and (9′) would be: when $t \geq t_0$, $C_{\mathrm{P}} = 0$. The obtained solutions are given in equations (22) and (22′) which are only valid under the condition that $t \geq t_0$:

$$\begin{aligned}\theta_{\mathrm{Pt-P}}^{t \geq t_0} = {} & \frac{1}{F_1^{t \geq t_0} F_2 + F_1^{t \geq t_0} B_2 + B_1 B_2} \\ & \times \left[F_1^{t \geq t_0} B_2 - \frac{a}{2Z^{t \geq t_0}} \right. \\ & \times \exp\left(- \frac{F_1^{t \geq t_0} + B_1 + F_2 + B_2 - Z^{t \geq t_0}}{2} (t - t_0) \right) \\ & - \frac{b}{2Z^{t \geq t_0}} \\ & \left. \times \exp\left(- \frac{F_1^{t \geq t_0} + B_1 + F_2 + B_2 + Z^{t \geq t_0}}{2} (t - t_0) \right) \right]\end{aligned} \tag{22}$$

$$\begin{aligned}\theta_{\mathrm{Pt-P'}}^{t \geq t_0} = {} & \frac{F_1^{t \geq t_0}}{2(F_1^{t \geq t_0} - B_2)(F_1^{t \geq t_0} F_2 + F_1^{t \geq t_0} B_2 + B_1 B_2)} \\ & \times \left[F_1^{t \geq t_0} F_2 (F_1^{t \geq t_0} - B_2) \right.\end{aligned}$$

$$+\left(\frac{F_1^{t\geq t_0}+B_1+F_2-B_2+Z^{t\geq t_0}}{2Z^{t\geq t_0}}\right)\times\exp\left(-\frac{F_1^{t\geq t_0}+B_1+F_2+B_2-Z^{t\geq t_0}}{2}(t-t_0)\right)+\left(\frac{F_1^{t\geq t_0}+B_1+F_2-B_2-Z^{t\geq t_0}}{2Z^{t\geq t_0}}\right)\times\exp\left(-\frac{F_1^{t\geq t_0}+B_1+F_2+B_2+Z^{t\geq t_0}}{2}(t-t_0)\right)\Bigg] \quad (22')$$

where

$$a=[\theta_{Pt-P}^{t=t_0}(F_1^{t\geq t_0}+B_1+F_2-B_2-Z^{t\geq t_0})+2\theta_{Pt-P'}^{t=t_0}(F_1^{t\geq t_0}-B_2)](F_1^{t\geq t_0}F_2+F_1^{t\geq t_0}B_2+B_1B_2)-2F_1^{t\geq t_0}F_2(F_1^{t\geq t_0}-B_2)-F_1^{t\geq t_0}B_2(F_1^{t\geq t_0}+F_2+B_1-B_2-Z^{t\geq t_0})$$

$$b=-[\theta_{Pt-P}^{t=t_0}(F_1^{t\geq t_0}+B_1+F_2-B_2+Z^{t\geq t_0})+2\theta_{Pt-P'}^{t=t_0}(F_1^{t\geq t_0}-B_2)](F_1^{t\geq t_0}F_2+F_1^{t\geq t_0}B_2+B_1B_2)+2F_1^{t\geq t_0}F_2(F_1^{t\geq t_0}-B_2)+F_1^{t\geq t_0}B_2(F_1^{t\geq t_0}+F_2+B_1-B_2+Z^{t\geq t_0})$$

$$F_1^{t\geq t_0}=AK_{8b}C_{P'}C_{H^+}^{q}\exp\left(\frac{-(1-\alpha_8)qF\eta_a}{RT}\right)$$

$$Z^{t\geq t_0}=\sqrt{(F_1^{t\geq t_0}+F_2+B_1-B_2)^2-4F_2(F_1^{t\geq t_0}-B_2)}$$

where $\theta_{Pt-P}^{t=t_0}$ and $\theta_{Pt-P'}^{t=t_0}$ are those surface coverage at $t=t_0$, which can be expressed by equations (11) and (11′) except that the time variable, t, in these two equations is replaced by t_0. $F_1^{t\geq t_0}$ is the F_1 value at $C_P=0$. If the product concentration ($C_{P'}$) produced by the contaminant oxidation is negligible, $F_1^{t\geq t_0}$ will be approximately equal to zero, and equations (22) and (22′) will become simpler. $Z^{t\geq t_0}$ is the Z value at $C_P=0$. The similar mathematical discussions to the equations (11) and (11′) for equations (22) and (22′) are listed in Appendix A.

For the special case that reaction (VII) does not exist, which corresponds to the case where the surface coverage of P′ is equal to zero, the surface coverage of P can be expressed by equation (23) at $t\geq t_0$:

$$\theta_{Pt-P}^{t\geq t_0}=\frac{1}{F_1^{t\geq t_0}+B_1}\{F_1^{t\geq t_0}-[F_1^{t\geq t_0}-\theta_{Pt-P}^{t=t_0}(F_1^{t\geq t_0}+B_1)]\times\exp(-(F_1^{t\geq t_0}+B_1)(t-t_0))\} \quad (23)$$

In the case that $C_{P'}=0$, which corresponds to that $F_1^{t\geq t_0}=0$, equation (23) simplifies to equation (24):

$$\theta_{Pt-P}^{t\geq t_0}=\theta_{Pt-P}^{t=t_0}\exp(-B_1(t-t_0)) \quad (24)$$

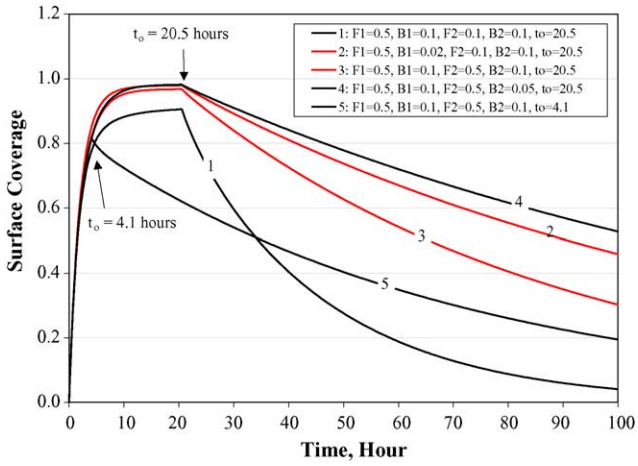

Fig. 7. Calculated surface coverage ($\theta_{Pt-P}+\theta_{Pt-P'}$) change before and after t_0 at various F_1, B_1, F_2, B_2 and t_0 values for the purpose of comparison. The units for those parameters are mol cm^{-2} h^{-1}, except for t_0 which is in hour. For the recovery process ($t\geq t_0$), F_1 is set to 0 for all cases.

Fig. 7 shows some calculated cases with various forward and backward reaction rate constants for the purpose of comparison.

The results show that the larger the reaction constant for the desorption of P on the surface (larger B_1), the faster the recovery rate would be (curve 1 versus curve 2). A larger reaction rate constant for the production of surface P′ (larger F_2) would make the recovery slower (curve 1 versus curve 3). For a larger B_2 (the rate constant for the surface electro-reduction of P′), the recovery process would become faster (curve 3 versus curve 4). Another observation from Fig. 7 is that the longer the contaminant exposure (longer t_0), the recovery process (curve 3 versus curve 5).

Combining equations (22) and (22′) with equations (14)–(16) allows the fuel cell voltage to be solved numerically for the recovery process. Fig. 8 shows the fuel cell voltage recovery at different contamination levels, t_0's, and current densities for the purpose of comparison. In the calculation, the contribution from reaction (VII) has been omitted. It is

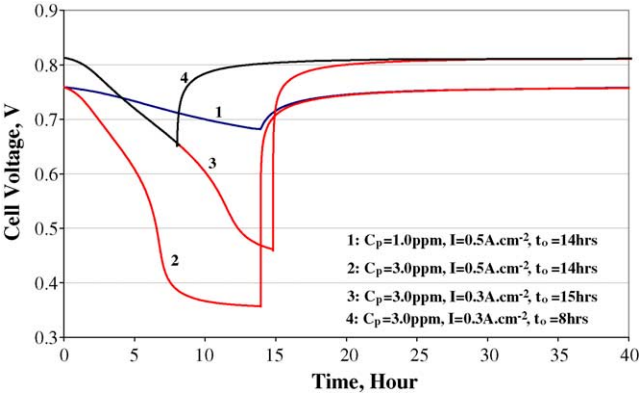

Fig. 8. Calculated fuel cell voltage recovery process at different levels of contaminant, current densities, and exposure times at 80 °C and 3.0 atm. The parameter values used for the calculation are those listed in Table 1. When $t\geq t_0$, F_1 is set to zero for all cases.

obvious from Fig. 8 that C_P, t_0, and current density can make a difference for the fuel cell voltage recovery process. A higher contaminant concentration (1 versus 2), a higher current density (2 versus 3), or a longer exposure (3 versus 4) make the recovery slower.

2.7. Temperature dependence of the contamination process

In general, temperature can affect the contamination process through its impact on the parameter values in the equations discussed previously. An increase in the temperature will cause a change in the magnitude of the reaction constants (k_{if} and k_{ib}) and other parameters such as solubility of hydrogen and contaminant in the electrolyte, their diffusion coefficients, hydrogen redox exchange current density, electrolyte resistance, and hydrogen surface recovery in the equilibrium state. For the contamination adsorption reactions (IV)–(VII), rising temperature will increase the magnitudes of the reaction rate constants in both directions. However, the backward reaction rate constants would be increased more than that of forward reaction rate constants, resulting in a slower contamination rate at higher temperature than that at lower temperature. At this stage, the quantitative approach for the temperature effect on the contamination process will not be pursued in this paper.

3. Conclusion

The model proposed in this paper for the anode poisoning process stems from the reaction mechanism for hydrogen oxidation on the platinum surface. In the mechanism of hydrogen oxidation, the dissociative chemical adsorption of adsorbed H_2 is considered as the rate-determining step for H_2 oxidation. The electrochemical reaction of dissociated H_2 following this rate-determining step is believed to have a Nernst behaviour from which the surface coverage of H_2, atomic H and unoccupied Pt sites are derived as a function of contaminant surface coverage. Chemical adsorption of contaminants on the platinum surface and their impact on the electrochemical hydrogen surface reaction are considered to be the main cause of the anode overpotential increase through the elimination of the active Pt catalyst sites.

The fuel cell current density expression as a function of anode and cathode overpotential is derived from the proposed reaction mechanism. The fuel cell performance degradation in the presence of feed stream contaminant(s) is formulated as a function of contaminant concentration, current density, and lifetime. The obtained equations can be used to simulate and estimate the chemical and electrochemical reaction rate constants, and make some prediction about the severity of the contamination and the performance recoverability.

Further work will be focused on modeling of the membrane and cathode poisoning processes and validating the models with more detailed experimental data.

Acknowledgement

The authors acknowledge the support of this research by the Institute for Fuel Cell Innovation (National Research Council Canada (NRC)). D.P.W. acknowledges the Natural Sciences and Engineering Research Council (NSERC) for Canada Research Chair support.

Appendix A

A.1. $t \le t_0$

The differential equations can be written as in equation (A.1) for the surface coverage:

$$\frac{d\theta_{Pt-P}}{dt} = -(F_1 + B_1 + F_2)\theta_{Pt-P} - (F_1 - B_2)\theta_{Pt-P'} + F_1$$
$$\frac{d\theta_{Pt-P'}}{dt} = (F_2\theta_{Pt-P} - B_2)\theta_{Pt-P'} \tag{A.1}$$

Regarding the initial conditions of that θ_{Pt-P} and $\theta_{Pt-P'}$ both equals to zero at $t = 0$, the analytical solutions for equation (A.1) can be obtained. Five cases have to be considered in order to avoid the solutions mathematically meaningless.

Case 1. $F_1 - B_2 \neq 0$, and $(F_1 + B_1 + F_2 - B_2)^2 + 4F_2(F_1 - B_2) \neq 0$. The analytical solutions are as in equation (A.2):

$$\theta_{Pt-P} = \frac{F_1}{F_1F_2 + F_1B_2 + B_1B_2}\left[B_2 - \frac{1}{2}\left(B_2 - \frac{F_1B_2 + B_1B_2 - B_2B_2 + 2F_1F_2 - F_2B_2}{Z}\right)\exp\left(-\frac{F_1 + B_1 + F_2 + B_2 - Z}{2}t\right)\right.$$
$$\left. - \frac{1}{2}\left(B_2 + \frac{F_1B_2 + B_1B_2 - B_2B_2 + 2F_1F_2 - F_2B_2}{Z}\right)\exp\left(-\frac{F_1 + B_1 + F_2 + B_2 + Z}{2}t\right)\right]$$
$$\theta_{Pt-P'} = \frac{F_1}{F_1F_2 + F_1B_2 + B_1B_2}\left[F_2 + \frac{1}{2}\left(B_2 - \frac{F_1B_2 + B_1B_2 - B_2B_2 + 2F_1F_2 - F_2B_2}{Z}\right)\left(\frac{F_1 + B_1 + F_2 - B_2 + Z}{2(F_1 - B_2)}\right)\right.$$
$$- \exp\left(-\frac{F_1 + B_1 + F_2 + B_2 - Z}{2}t\right) + \frac{1}{2}\left(B_2 + \frac{F_1B_2 + B_1B_2 - B_2B_2 + 2F_1F_2 - F_2B_2}{Z}\right)$$
$$\left. - \left(\frac{F_1 + B_1 + F_2 - B_2 - Z}{2(F_1 - B_2)}\right)\exp\left(-\frac{F_1 + B_1 + F_2 + B_2 + Z}{2}t\right)\right] \tag{A.2}$$

where $Z = ((F_1 + B_1 + F_2 - B_2)^2 + 4F_2(F_1 - B_2))^{1/2}$

Case 2. $F_1 - B_2 \neq 0$, $B_1 = 0$ and $F_1 = F_2 + B_2$. The solutions are as in equation (A.3):

$$\theta_{\mathrm{Pt-P}} = \frac{1}{F_1}[F_1 + F_2 - (F_1 + F_2 - F_1F_2t)\ \exp(-F_1t)]$$
$$\theta_{\mathrm{Pt-P'}} = \frac{F_2}{F_1}[1 - (1 + F_1t)\ \exp(-F_1t)] \tag{A.3}$$

Case 3. $F_1 - B_2 \neq 0$, $F_2 = 0$ and $B_2 = F_1 + B_1$. The solutions are as in equation (A.4):

$$\theta_{\mathrm{Pt-P}} = \frac{F_1}{F_1 + B_1}[1 - \exp(-(F_1 + B_1)t)]$$
$$\theta_{\mathrm{Pt-P'}} = 0 \tag{A.4}$$

Case 4. $F_1 - B_2 = 0$ and $B_1 + F_2 \neq 0$. The solutions are as in equation (A.5):

$$\theta_{\mathrm{Pt-P}} = \frac{F_1}{F_1 + B_1 + F_2}[1 - F_1\ \exp(-(F_1 + B_1 + F_2)t)]$$
$$\theta_{\mathrm{Pt-P'}} = \frac{F_2}{F_1 + B_1 + F_2} \times \left[1 + \frac{F_1}{F_2 + B_1}\ \exp(-(F_1 + B_1 + F_2)t)\right] - \frac{F_1 + B_1 + F_2}{F_2 + B_1}\ \exp(-F_1t)] \tag{A.5}$$

Case 5. $F_1 - B_2 = 0$ and $B_1 + F_2 = 0$. The solutions are as in equation (A.6):

$$\theta_{\mathrm{Pt-P}} = 1 - \exp(-F_1t)]$$
$$\theta_{\mathrm{Pt-P'}} = 0 \tag{A.6}$$

A.2. $t \geq t_0$

The differential equations are the same as those expressed by equation (A.1). However, the boundary conditions for solving the differential equations are different. The boundary condition would be: if $t \geq t_0$, $C_{\mathrm{P}} = 0$ and $\theta_{\mathrm{Pt-P}} = \theta_{\mathrm{Pt-P}}^{t \leq t_0}$ and $\theta_{\mathrm{Pt-P'}} = \theta_{\mathrm{Pt-P'}}^{t=t_0}$.

The analytical solutions for equation (A.1) can be obtained and five cases have to be considered in order to avoid the solution mathematical meaningless. Note that the obtained equations listed below are only valid when the time is longer than t_0.

Case 1. $F_1 - B_2 \neq 0$, and $(F_1 + B_1 + F_2 - B_2)^2 + 4F_2(F_1 - B_2) \neq 0$. The analytical solutions are as in equation (A.7):

$$\theta_{\mathrm{Pt-P}}^{t \geq t_0} = \frac{1}{F_1^{t \geq t_0}F_2 + F_1^{t \geq t_0}B_2 + B_1B_2}\left[F_1^{t \geq t_0}B_2 - \frac{a}{2Z^{t \geq t_0}}\ \exp\left(-\frac{F_1^{t \geq t_0} + B_1 + F_2 + B_2 - Z^{t \geq tO}}{2}(t - t_0)\right) - \frac{b}{2Z^{t \geq t_0}} \times \exp\left(-\frac{F_1^{t \geq t_0} + B_1 + F_2 + B_2 + Z^{t \geq t_0}}{2}(t - t_0)\right)\right]$$

$$\theta_{\mathrm{Pt-P'}}^{t \geq t_0} = \frac{F_1^{t \geq t_0}}{2(F_1^{t \geq t_0} - B_2)(F_1^{t \geq t_0}F_2 + F_1^{t \geq t_0}B_2 + B_1B_2)}\left[F_1^{t \geq t_0}F_2(F_1^{t \geq t_0} - B_2) + \left(\frac{F_1^{t \geq t_0} + B_1 + F_2 - B_2 + Z^{t \geq t_0}}{2Z^{t \geq t_0}}\right) \times \exp\left(-\frac{F_1^{t \geq t_0} + B_1 + F_2 + B_2 - Z^{t \geq t_0}}{2}(t - t_0)\right) + \left(\frac{F_1^{t \geq t_0} + B_1 + F_2 - B_2 - Z^{t \geq t_0}}{2Z^{t \geq t_0}}\right) \times \exp\left(-\frac{F_1^{t \geq t_0} + B_1 + F_2 + B_2 + Z^{t \geq t_0}}{2}(t - t_0)\right)\right] \tag{A.7}$$

where

$$a = [\theta_{\mathrm{Pt-P}}^{t=t_0}(F_1^{t \geq t_0} + B_1 + F_2 - B_2 - Z^{t \geq t_0}) + 2\theta_{\mathrm{Pt-P'}}^{t=t_0}(F_1^{t \geq t_0} - B_2)](F_1^{t \geq t_0}F_2 + F_1^{t \geq t_0}B_2 + B_1B_2) - 2F_1^{t \geq t_0}F_2(F_1^{t \geq t_0} - B_2) - F_1^{t \geq t_0}B_2(F_1^{t \geq t_0} + F_2 + B_1 - B_2 - Z^{t \geq t_0})$$

$$b = -[\theta_{\mathrm{Pt-P}}^{t=t_0}(F_1^{t \geq t_0} + B_1 + F_2 - B_2 + Z^{t \geq t_0}) + 2\theta_{\mathrm{Pt-P'}}^{t=t_0}(F_1^{t \geq t_0} - B_2)](F_1^{t \geq t_0}F_2 + F_1^{t \geq t_0}B_2 + B_1B_2) + 2F_1^{t \geq t_0}F_2(F_1^{t \geq t_0} - B_2) + F_1^{t \geq t_0}B_2(F_1^{t \geq t_0} + F_2 + B_1 - B_2 + Z^{t \geq t_0})$$

$$F_1^{t \geq t_0} = AK_{8\mathrm{b}}C_{\mathrm{P'}}C_{\mathrm{H^+}}^{q}\ \exp\left(\frac{-(1 - \alpha_8)qF\eta_{\mathrm{a}}}{RT}\right)$$

$$Z^{t \geq t_0} = \sqrt{(F_1^{t \geq t_0} + F_2 + B_1 - B_2)^2 - 4F_2(F_1^{t \geq t_0} - B_2)}$$

$\theta_{Pt-P}^{t=t_0}$ and $\theta_{Pt-P'}^{t=t_0}$ are those surface coverage at $t = t_0$, which can be expressed by equations (18) and (18′) except that the time t's in these two equations are replaced by t_0's. $F_1^{t\geq t_0}$ is the F_1 value at $C_P = 0$ and $Z^{t\geq t_0}$ is the Z value at $C_P = 0$.

Case 2. $F_1 - B_2 \neq 0$, $B_1 = 0$ and $F_1 = F_2 + B_2$. The solutions are as in equation (A.8):

$$\theta_{Pt-P}^{t\geq t_0} = 1 - \frac{F_2}{F_1^{t\geq t_0}} + \left[\theta_{Pt-P}^{t=t_0} - \frac{F_2}{F_1^{t\geq t_0}} - 1 - F_2(\theta_{Pt-P}^{t=t_0} + \theta_{Pt-P'}^{t=t_0} - 1)(t - t_0)\right] \exp(-F_1^{t\geq t_0}(t - t_0))$$

$$\theta_{Pt-P'}^{t\geq t_0} = \frac{F_2}{F_1^{t\geq t_0}} + \left[\theta_{Pt-P'}^{t=t_0} - \frac{F_2}{F_1^{t\geq t_0}} + F_2(\theta_{Pt-P}^{t=t_0} + \theta_{Pt-P'}^{t=t_0} - 1) \times (t - t_0)\right] \exp(-F_1^{t\geq t_0}(t - t_0)) \quad \text{(A.8)}$$

Case 3. $F_1 - B_2 \neq 0$, $F_2 = 0$ and $B_2 = F_1 + B_1$. The solutions are as in equation (A.9):

$$\theta_{Pt-P}^{t\geq t_0} = 1 - \frac{1}{F_1^{t\geq t_0} + B_1} + \theta_{Pt-P'}^{t=t_0} \exp(-F_1^{t\geq t_0}(t - t_0)) + \left(\theta_{Pt-P}^{t=t_0} - \theta_{Pt-P'}^{t=t_0} - \frac{F_1^{t\geq t_0}}{F_1^{t\geq t_0} + B_1}\right) \exp \times (-(F_1^{t\geq t_0} + B_1)(t - t_0)) \quad \text{(A.9)}$$

$$\theta_{Pt-P'}^{t\geq t_0} = \theta_{Pt-P'}^{t=t_0} \exp(-F_1^{t\geq t_0}(t - t_0))$$

Case 4. $F_1 - B_2 = 0$ and $B_1 + F_2 \neq 0$. The solutions are as in equation (A.10):

$$\theta_{Pt-P}^{t\geq t_0} = \frac{F_1^{t\geq t_0}}{F_1^{t\geq t_0} + B_1 + F_2} + \left(\theta_{Pt-P}^{t=t_0} - \frac{F_1^{t\geq t_0}}{F_1^{t\geq t_0} + B_1 + F_2}\right) \exp(-(F_1^{t\geq t_0} + B_1 + F_2)(t - t_0))$$

$$\theta_{Pt-P'}^{t\geq t_0} = \frac{F_2}{F_1^{t\geq t_0} + B_1 + F_2} + \left(\theta_{Pt-P'}^{t=t_0} + \frac{F_2(\theta_{Pt-P}^{t=t_0} - 1)}{B_1 + F_2}\right) \exp(-F_1^{t\geq t_0}(t - t_0)) - \frac{F_2}{B_1 + F_2} \times \left(\theta_{Pt-P}^{t=t_0} - \frac{F_1^{t\geq t_0}}{F_1^{t\geq t_0} + B_1 + F_2}\right) \exp(-(F_1^{t\geq t_0} + B_1 + F_2)(t - t_0)) \quad \text{(A.10)}$$

Case 5. $F_1 - B_2 = 0$ and $B_1 + F_2 = 0$. The solutions are as in equation (A.11):

$$\theta_{Pt-P}^{t\geq t_0} = 1 + (\theta_{Pt-P}^{t=t_0} - 1) \exp(-F_1^{t\geq t_0}(t - t_0))$$

$$\theta_{Pt-P'}^{t\geq t_0} = \theta_{Pt-P'}^{t=t_0} \exp(-F_1^{t\geq t_0}(t - t_0)) \quad \text{(A.11)}$$

References

[1] P.R. Hayter, P. Mitchell, R.A.J. Dams, C. Dudfield, N. Gladding, The effect of contaminants in the fuel and air streams on the performance of a solid polymer fuel cell, Contract Report (ETSU F/02/00126/REP), Wellman CJB Limited, Portsmouth, UK, 1997.

[2] F.A. Uribe, S. Gottesfeld, T.A. Zawodzinski Jr., J. Electrochem. Soc. 149 (3) (2002) 293–296.

[3] F.A. Uribe, T.A. Zawodzinski, Jr., ECS Meeting Abstracts, No. 339, San Fracisco, 2001.

[4] D.C. Papageorgopoulos, F.A. de Bruijn, J. Electrochem. Soc. 149 (2) (2002) A140–A145.

[5] J.M. Moore, P.L. Adcock, J.B. Lakeman, G.O. Mepsted, J. Power Sources 85 (2000) 254–260.

[6] F.A. de Bruijn, D.C. Papageorgopoulos, E.F. Sitters, G.J.M. Janssen, J. Power Sources 110 (2002) 117–124.

[7] Z.G. Qi, C.Z. He, A. Kaufman, J. Power Sources 111 (2002) 239–247.

[8] G. Mepsted, Investigation of the effects of air contaminations on SPFC performance, Contract Technical Report (ETSU-F-02/00172/Rep), Defence and Evaluation Research Agency, UK, 2001.

[9] Y. Kamiya, K. Narusawa, M. Hayashida, Proceedings of the 17 International Electric Vehicle Symposium and Exposition: Driving New Vision, 2000, pp. 1–9.

[10] J. St-Pierre, D.P. Wilkinson, S. Knights, M.L. Bos, J. New Mater. Electrchem. Syst. 3 (2) (2000) 99–106.

[11] T. Okada, N. Nakamura, M. Yuasa, I. Sekine, J. Power Sources 144 (8) (1997) 2744–2750.

[12] N.J. Maskalick, Proceeding of the Joint Contractors Meeting: FE/EE Advanced Turbine Systems Conference FE Fuel Cells and Coal-fired Heat Engines Conference, 1993, pp. 313–322.

[13] J.C. Amphlett, R.M. Baumert, R.F. Mann, B.A. Peppley, P.R. Roberge, A. Rodrigues, 206th ACS National Meeting, 1993, p. 530.

[14] S.M. Park, T.J. O'Brien, Effects of several trace contaminants on fuel cell performance, Technical Report (# DOE/METC/RI-80/16), Department of Energy, Morgantown, WV, USA, 1980.

[15] T. Okada, J. Electroanal. Chem. 465 (1) (1999) 1–29 (Parts I & II).

[16] K. Mitsuda, H. Miyoshi, M. Matsumoto, K. Usami, Denki Kagaku 62 (9) (1994) 775–783.

[17] R.W. Lyczkowski, D. Gidaspow, AlChE J. 17 (5) (1974) 1208–1214.

[18] D.T. Chin, P.D. Howard, J. Electrochem. Soc. 133 (12) (1986) 2447–2450.

[19] A. Heinzel, W. Benz, F. Mahlendort, O. Niemzig, J. Roes, 2002 Fuel Cell Seminar Abstracts, Palm Springs, CA, 2002, pp. 149–152.

[20] P.J. de Wild, R.G. Nyqvist, F.A. de Bruijn, 2002 Fuel Cell Seminar Abstract, Palm Springs, CA, 2002, pp. 227–230.

[21] T. Nakatsu, A. Fukuda, K. Furuie, Hokkaido Denryoku Kenkyu Nenpo 30 (1999) 61–67.

[22] L.G. Marianowski, H. Shimotake, Progress in Batteries and Solar Cells, vol. 5, JEC Press Inc., 1984, pp. 283–289.

[23] R.J. Remick, E.H.V. Camara, Electrochem. Soc. Extended Abstr. 84–2 (1984) 88.

[24] P.N. Ross Jr., Technical Report (US Contract/Grant #DOE AC03-76SF00098, Report #LBL–18001), Lawrence Berleley Lab., CA, 1985.

[25] P. Stonehart, G. Kohlmayr, Electrochim. Acta 17 (1972) 369–382.

[26] W. Vogel, J. Lundquist, P. Ross, P. Stonehart, Electrochim. Acta 20 (1975) 79–93.

[27] T. Tada, in: W. Vielstich, H.A. Gasteiger, A. Lamm (Eds.), Handbook of Fuel Cells—Fundamental, Technology and Application, vol. 3, John Wiley & Sons, 2003, Chapter 38.
[28] T.E. Springer, T. Rockward, T.A. Zawodzinski, S. Gottesfeld, J. Electrochem. Soc., 148(1) (2110) A11-A23.
[29] S.H. Chan, S.K. Goh, S.P. Jiang, Electrochim. Acta 48 (2003) 1905–1919.
[30] K.K. Bhatia, C.Y. Wang, Electrochim. Acta 49 (2004) 2333–2341.
[31] R. Delevie, in: P. Delahay (Ed.), Advances in Electrochemistry and Electrochemical Engineering, vol. 6, Interscience Publishers, New York, 1967, p. 329.
[32] J. Giner, C. Hunter, J. Electrochem. Soc. 116 (1969) 1124–1130.
[33] W. Vogel, J. Lundquist, A. Bradford, Electrochim. Acta 17 (1972) 1735–1744.
[34] T.E. Springer, I.D. Raistrick, J. Electrochem. Soc. 136 (1989) 1594–1603.
[35] M. Watanabe, H. Igarashi, K. Yosioka, Electrochim. Acta 40 (3) (1995) 329–334.
[36] J.P. Hoare, in: A.J. Bard (Ed.), Encyclopedia of Electrochemistry of the Elements, vol. II, Marcel Dekker, New York, 1971, Chapter 5.
[37] K. Kinoshita, Electrochemical Oxygen Technology, John Wiley & Sons, New York, 1992, Chapter 2.
[38] EG&G Services, Parsons Inc., Science Applications International Corp., Fuel Cell Hand book, DOE Contract #DE-AM26-99FT40575, DOE, West Virginia, 2000 (Chapter 2).
[39] T. Erdey-Gruz, M. Volmer, Z. Physik. Chem. 150A (1930) 203.
[40] J. Tafel, Z. Physik. Chem. 50 (1905) 641.
[41] K.J. Veter, Electrochemical Kinetics, Academic Press, New York, 1967, p. 519.
[42] J. Heyrovski, Res. Trav. Chim. Pays-Bas 46 (1927) 582.
[43] V.S. Bagotzky, N.V. Osetrova, Electroanal. Chem. Interfacial Electrochem. 43 (1973) 233–249.
[44] P.N. Ross, P. Stonehart, J. Res. Inst. Catalysis, Hokkaido Univ. 22 (1) (1974) 22–41.
[45] T.R. Ralph, G.A. Hards, J.E. Keating, S.A. Campbell, D.P. Wilkinson, M. Davis, J. St-Pierre, M.C. Johnson, J. Electrochem. Soc. 144 (1997) 3845–3857.
[46] H.F. Oetjen, V.M. Schmidt, U. Stimming, F. Trila, J. Electrochem. Soc. 143 (1996) 3838–3842.